Dosimetry Modeling of Inhaled Formaldehyde: Comparisons of Local Flux Predictions in the Rat, Monkey, and Human Nasal Passages

J. S. Kimbell,[1] R. P. Subramaniam,[2] E. A. Gross, P. M. Schlosser, and K. T. Morgan[3]

CIIT Centers for Health Research, P.O. Box 12137, 6 Davis Drive, Research Triangle Park, North Carolina 27709

Formaldehyde-induced nasal squamous cell carcinomas in rats and squamous metaplasia in rats and rhesus monkeys occur in specific regions of the nose with species-specific distribution patterns. Experimental approaches addressing local differences in formaldehyde uptake patterns and dose are limited by the resolution of dissection techniques used to obtain tissue samples and the rapid metabolism of absorbed formaldehyde in the nasal mucosa. Anatomically accurate, 3-dimensional computational fluid dynamics models of F344 rat, rhesus monkey, and human nasal passages were used to estimate and compare regional inhaled formaldehyde uptake patterns predicted among these species. Maximum flux values, averaged over a breath, in nonsquamous epithelium were estimated to be 2620, 4492, and 2082 pmol/(mm^2-h-ppm) in the rat, monkey, and human respectively. Flux values predicted in sites where cell proliferation rates were measured as similar in rats and monkeys were also similar, as were fluxes predicted in a region of high tumor incidence in the rat nose and the anterior portion of the human nose. Regional formaldehyde flux estimates are directly applicable to clonal growth modeling of formaldehyde carcinogenesis to help reduce uncertainty in human cancer risk estimates.

Key Words: formaldehyde; nasal uptake; computational fluid dynamics; F344 rat; rhesus monkey; human; nasal passages.

Inhaled formaldehyde induces squamous cell carcinomas in the nasal passages of rats and squamous metaplasia in rat and monkey nasal epithelium (Kerns *et al.,* 1983; Monticello *et al.,* 1989). These and other lesions occur in specific sites with species-specific patterns of lesion distribution (Monticello *et al.,* 1989, 1996; Morgan *et al.,* 1986b). Site-specificity of formaldehyde-induced lesions in rats and monkeys implicates regional tissue susceptibility and dose as factors potentially contributing to tissue damage. The observation that lesions occur only in areas normally lined by epithelial types other than the squamous type suggests that these regions may be more susceptible to damage from formaldehyde than areas normally lined by squamous epithelium. Species-specific patterns of lesions in rats and monkeys suggest that regional dose is a factor.

Regional dose is a function of the amount of formaldehyde delivered by inhaled air and the absorption characteristics of the nasal lining. The amount delivered by inhaled air depends on major airflow patterns, air-phase diffusion, and absorption at the air-lining interface. The dose of formaldehyde to cells depends on the amount absorbed at the air-lining interface, mucus-to-tissue phase diffusion, chemical interactions such as reactions and solubility, and clearance rates. Species differences in these factors are determinants of species-specific lesion distributions.

Experimental approaches to address regional differences in formaldehyde uptake patterns and tissue dose are limited by the resolution of dissection techniques used to obtain tissue samples from different sites in rat nasal epithelium and the labile nature of formaldehyde absorbed by these tissues (Heck *et al.,* 1990). In the rat nose, no more than 2 or 3 dissection sites can typically be separated from each other and this procedure necessitates 3 to 5 min of careful dissection. In addition, there is a need to relate the amount of inhaled gas delivered to different sites in the nose to biomarkers of dose or effect such as formaldehyde-induced DNA–protein cross-links (DPX; Casanova *et al.,* 1989, 1991, 1994) and regional cell proliferation rates (Monticello *et al.,* 1989, 1991). If inhaled gas uptake could be predicted throughout the nasal passages, then relationships between gas uptake and rates of DPX formation and cell proliferation would allow DPX and cell proliferation data to be interpolated from measurement sites to the rest of the nasal passage. This information would be useful for estimating cell birth, death, and mutation rates in clonal growth models for carcinogenesis (Cohen and Ellwein, 1990; Moolgavkar and Venzon, 1979).

To estimate regional uptake of inhaled gas in the nose, 3-dimensional, anatomically accurate computational fluid dynamics (CFD) models of rat, monkey, and human nasal airflow (Kepler *et al.,* 1998; Kimbell *et al.,* 1997a; Subramaniam *et al.,* 1998) and inhaled gas uptake (Kepler *et al.,* 1998; Kimbell *et al.,* 1993, 1997b) were developed. To confirm formaldehyde

---

uptake simulations, the rat and monkey CFD models were used in conjunction with physiologically based pharmacokinetic (PBPK) models to predict regional nasal DPX (Cohen Hubal *et al.,* 1997; Conolly *et al.,* 2000). In the approach used by Cohen Hubal and colleagues, PBPK model parameters were either fixed from actual measurements or estimated by fitting the rat PBPK model to DPX measured in nasal mucosa taken from the entire respiratory epithelial area of formaldehyde-exposed rats. Optimizations used a (non-CFD) formaldehyde flux value that was calculated from a nasal surface area estimate and nasal uptake that was experimentally measured for the entire rat nasal passages. The PBPK model was then used to predict DPX that would occur in a specific site within the respiratory epithelium (the high tumor region) using a formaldehyde flux value provided for that region by the rat CFD model described by Kimbell *et al.* (1993). Predictions were in good agreement with experimental measurements of DPX in the high tumor region of rats exposed to inhaled formaldehyde.

Conolly and coworkers extended these results to both high and low tumor regions in the rat using regional formaldehyde flux estimates from an improved rat CFD model described by Kimbell *et al.* (1997a). The PBPK model was able to predict low tumor DPX with parameters that were fitted to high tumor data alone. Parameters fitted to low tumor data alone were similar to those fitted to high tumor data alone. These results provided further support that site-specific estimates of formaldehyde flux from the CFD modeling approach were adequate for predicting site-specific DPX.

The CFD models provide a means for estimating the amount of inhaled gas reaching any site along nasal passage walls. Such estimates can be used to test hypotheses about mechanisms of toxicity as well as to supply information for risk assessment. For example, the CFD models were used to provide support for the hypothesis that the distribution of formaldehyde-induced squamous metaplasia in the rat nasal passages is related to the location of high-flux regions posterior to squamous epithelium (Kimbell *et al.,* 1997b). Results from CFD modeling supported the hypothesis that interspecies differences in uptake patterns along airway walls, influenced by differing nasal airflow characteristics, account for differing distributions of formaldehyde-induced lesions in rats and primates (Kepler *et al.,* 1998; Kimbell *et al.,* 1993). The CFD models were also used to estimate the surface area and volume of specific anatomical features (Bogdanffy *et al.,* 1998; Frederick *et al.,* 1998), the allocation of inspired air to specific flow streams (Andersen *et al.,* 1999; Bush *et al.,* 1998; Frederick *et al.,* 1998), and gas phase mass transfer coefficients (Frederick *et al.,* 1998) for use in predicting human risks from inhaled gases.

The purpose of the present work was to (1) make predictions of formaldehyde flux in the entire nasal passages of rats, monkeys, and humans, (2) estimate flux in specific sites for correlation with formaldehyde-induced cell proliferation data, and (3) compare flux predictions among the 3 species. Flux patterns predicted using CFD models have been reported in the anterior rat nasal passages for ozone (Cohen Hubal *et al.,* 1996) and reactive, water-soluble gases like formaldehyde (Cohen Hubal *et al.,* 1997; Kimbell *et al.,* 1993, 1997b). Predicted flux patterns were also described in the rhesus monkey nasal passages for a formaldehyde-like gas (Kepler *et al.,* 1998). Formaldehyde flux predicted in sites where DPX were measured in formaldehyde-exposed rats and monkeys was reported by Conolly and colleagues (Conolly *et al.,* 2000).

This paper describes predicted formaldehyde uptake in the entire rat, monkey, and human nasal passages using improved estimates of uptake conditions at the interface between air and tissue that differentiate between mucus-coated and nonmucus-coated tissue. Estimates of formaldehyde flux in sites where cell proliferation rates were measured in formaldehyde-exposed rats and monkeys are provided. Interspecies comparisons of predicted regional flux, such as maximum values and flux in lesion sites, are made.

METHODS

Regional flux of formaldehyde from inhaled air to the air-lining interface was estimated from CFD simulations of airflow and formaldehyde uptake that were conducted using 3-dimensional, anatomically accurate reconstructions of the nasal passages of an adult male F344 rat, rhesus monkey, and human. The construction of the CFD models and the simulation of steady-state inspiratory nasal airflow were previously described in detail (Kepler *et al.,* 1998; Kimbell *et al.,* 1993, 1997a; Subramaniam *et al.,* 1998).

Assumptions

Anatomical assumptions. Rat and monkey nasal cavities were assumed to be symmetrical so CFD models were constructed for 1 side of the nose for both of these species. Surface areas and volumes from the rat and monkey CFD models were doubled to account for both sides of the nasal passages. The human CFD model included both sides; a surface area adjustment was not needed for results from this model. The nasal passages of all 3 species were assumed to have a continuous mucus coating over all surfaces except specific areas in the nasal vestibule (see below; demonstrated for the rat by Morgan *et al.,* 1984). Each CFD model was assumed to be anatomically representative for its species.

Airflow assumptions. The major patterns of inhaled airflow simulated at steady state were assumed to be similar to those occurring during resting breathing (based on calculation of the Strouhal number; see Subramaniam *et al.,* 1998). The lack of flexible nasal walls, mucus movement, nasal hairs, and gain or loss of heat or humidity in the CFD models was assumed to contribute insignificantly to error in airflow simulations.

Formaldehyde uptake assumptions. Although formaldehyde uptake is probably affected by the presence of other inhaled species, by the presence of water vapor, and by normal, cyclic changes in nasal airway patency (the nasal cycle), these effects were not taken into account in the formaldehyde uptake simulations presented here. In particular, these simulations were assumed to represent average uptake over the nasal cycle. Throughout this article, flux values also represent an estimated average over the breathing cycle. Since formaldehyde is a highly water soluble and reactive gas, formaldehyde concentration in respired air during exhalation was assumed to be negligible. Therefore flux into nasal passage walls during exhalation was assumed to be 0 for each breath. Inspiratory and expiratory phases of the breathing cycle were assumed to take equal amounts of time so that flux values were derived by halving estimates obtained from the steady-state inspiratory CFD models.

The air-phase diffusivity of formaldehyde (D_{AB}) was assumed to be constant throughout the nasal passages of all three species. A value of 0.15 cm²/sec for D_{AB} was estimated using the following formula referenced by Hobler (1966):

$$D_{AB} = \frac{0.602\ T^{1.78}(1 + \sqrt{M_A + M_B})}{P(v_A^{1/3} + v_B^{1/3})^2 \sqrt{M_A M_B}} \text{ cm}^2/\text{sec}$$

where T is the temperature in degrees Kelvin (298°), M_A is the molecular weight of air in kg/kg-mole (28.8), Mbyte is the molecular weight of formaldehyde (30), P is the total pressure in mm Hg (760), v_A is the molar volume of air at the normal boiling point in cm³/g-mole (29.9; Hobler, 1966), and v_B is the molar volume of formaldehyde (estimated to be 29.6 from summing up the values of the atomic volumes as in Hobler, 1966).

The rate of formaldehyde transport into tissue was assumed to far exceed mucus velocity rates (Morgan *et al.,* 1986a), so that mucus transport of formaldehyde was not included in the CFD models. The rate of formaldehyde absorption at air-lining interfaces was assumed to be proportional to the air-phase formaldehyde concentration adjacent to the nasal-lining layer. The value of the proportionality constant, or mass transfer coefficient, depended on whether or not the nasal lining was mucus-coated. In rats, monkeys, and humans, nonmucus-coated epithelium is located in the nasal vestibule and is of the squamous type. A mass transfer coefficient for nonmucus-coated squamous epithelium was estimated from measurements of formaldehyde absorption made for human epidermal tissue (see below). The rest of the nasal passages in all 3 species were assumed to be coated by mucus. A mass transfer coefficient for mucus-coated regions in the monkey and human was assumed to be the same as the value obtained for the rat by fitting overall formaldehyde uptake predictions in the rat to formaldehyde uptake data measured in the rat (Patterson *et al.,* 1986).

Computational meshes and airflow simulations. The rat and monkey CFD models were constructed from tracings of airway outlines of the right nasal passages from the nostril to the nasopharynx from serial-step sections of embedded tissue specimens as described by Kimbell *et al.* (1993) and Kepler *et al.* (1995). The human model was constructed from airway tracings of both sides of the nasal passages from the nostril through the nasopharynx from magnetic resonance image scans as described by Subramaniam *et al.* (1998). The CFD models were created using in-house software (Godo *et al.,* 1995) and the finite element mesh preprocessor of the computational fluid dynamics software package FIDAP (Fluent Inc., Lebanon, NH). Resulting meshes were designed to have elements as uniform in shape and size as anatomy allowed.

The location and extent of nonmucus-coated regions in the nasal vestibules of each species were estimated from descriptions by Morgan and colleagues (Morgan *et al.,* 1984), Harkema and colleagues (Harkema, 1992; Harkema *et al.,* 1987), and Mygind and colleagues (Mygind *et al.,* 1982). The location of squamous epithelium in the rat and monkey nasal vestibule was determined by light microscopy and was approximated in the human from the description by Mygind and colleagues (1982). The approximate locations of squamous and mucus- and nonmucus-coated epithelia were mapped onto the reconstructed nasal geometry of the CFD models. In all 3 species, the mucus- and nonmucus-coated regions taken together comprised the entire surface area of the nasal passages.

In the rat and monkey, the locations of areas in which cell proliferation rates were measured (Monticello *et al.,* 1989, 1996) were also mapped into the CFD models. In the rat, these areas were the anterior lateral meatus, the posterior lateral meatus, the anterior mid-septum, the anterior dorsal septum, and the medial maxilloturbinate. In the monkey, these areas were cross sections corresponding to Levels A, B, C, D, and E as described by Monticello *et al.* (1989).

Steady-state airflow simulations required the numerical solution of the Navier-Stokes equations of motion for incompressible Newtonian fluid flow (Batchelor, 1967). FIDAP was used to solve these equations in the 3 nasal geometries as described by Kimbell *et al.* (1997a), Kepler *et al.* (1998), and Subramaniam *et al.* (1998). To calculate an airflow rate that would be comparable among species, the amount of inspired air (tidal volume, V_T) was
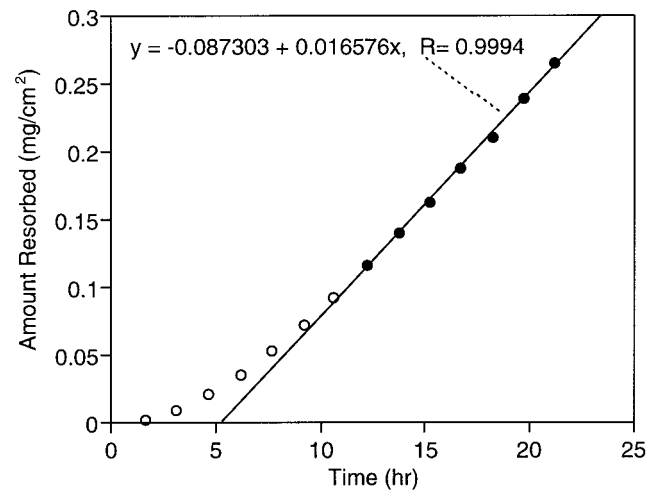

FIG. 1. Penetration of formaldehyde through skin *ex vivo*. Line fitted to filled circles. Data from Lodén (1986).

divided by the estimated time involved in inhalation (half the time a breath takes, or (1/2)(1/[breathing frequency, f]). Thus, an inspiratory flow rate was calculated to be 2 V_T f, or twice the minute volume. Minute volumes were allometrically scaled to 0.288 l/min for a 315 g rat from data given by Mauderly (1986), allometrically scaled to 2.4 l/min for an 11.9 kg monkey from a formula described by Guyton (1947), and 7.4 l/min in the human, approximating ventilatory rates for resting breathing (ICRP66, 1994). Simulations were therefore carried out at 0.576 l/min, 4.8 l/min, and 15.0 l/min in the rat, monkey, and human, respectively. Airflow simulations compared well with descriptions and measurements of flow in nasal molds for each species (Kepler *et al.,* 1998; Kimbell *et al.,* 1993, 1997a; Subramaniam *et al.,* 1998).

Uptake Simulations

Boundary conditions. Two pieces of information were needed to conduct simulations of regional uptake of formaldehyde by nasal walls in each species: (1) airflow velocities, supplied by the simulations described above, and (2) boundary conditions for transport of inhaled formaldehyde at airway walls. The latter refer to conditions imposed *a priori* on the concentration of formaldehyde at the nostril surface and on the transport rate (flux) of formaldehyde at the interface between air and the airway lining. Formaldehyde uptake simulations were run for an inhaled concentration of 1 ppm in each species. Predictions for other inhaled concentrations can be obtained by multiplying the results presented here by the desired concentration in ppm. Constants of proportionality between formaldehyde flux and the air phase concentration of formaldehyde near the wall were determined separately for nonmucus-coated squamous epithelium located in the nasal vestibule and for the rest of the nose in each species as follows.

Mass transfer coefficient for nonmucus-coated epithelium. Uptake of inhaled formaldehyde by the nonmucus-coated squamous epithelium located in the nasal vestibule of all 3 species was assumed to be similar to uptake determined by Lodén (1986) in experiments measuring formaldehyde transport through human epidermal tissue. In this work, Lodén mounted pieces of full-thickness skin in a diffusion flow-cell, with medium containing formaldehyde on 1 side of the cell and receptor media continuously pumped through the other side of the cell (keeping formaldehyde concentration close to 0 on the receptor side). Mean values for the total amount of formaldehyde resorbed (taken up by the receptor medium) from a 10% formalin solution are shown in Figure 1. A subset of these data in the steady-state portion of the curve was selected visually (filled circles in Fig. 1), and linear regression was used to fit a line through these points to estimate formaldehyde resorbed per h at steady state (see below).

The density of formaldehyde is 0.815 g/ml, so the concentration in a 10% v/v solution is C = 81.5 mg/cm^3. The concentration of formaldehyde in the skin on the side in contact with this solution was assumed to be C · K$_{s:w}$, where K$_{s:w}$ is the equilibrium partition coefficient for formaldehyde between skin and water ([HCHO]$_{skin}$/[HCHO]$_{water}$ at equilibrium). Since the receptor side was kept flushed, the concentration in the skin on that side was assumed to be 0. Measurements of ^{14}C-formaldehyde activity in the skin at the end of the experiment showed a clear gradient from the exposed side to the receptor side, with the concentration on the receptor side being less than 2% of that on the exposed side, indicating that this was a good assumption. The driving force for diffusion across the skin is thus F = (C − 0) · K$_{s:w}$ = C · K$_{s:w}$.

The resistance to diffusion, R, is the ratio between the thickness of the layer of skin and the diffusivity. Thus, R = d$_s$/D$_{skin}$, where d$_s$ is the skin thickness and D$_{skin}$ is the diffusivity in the skin. The skin used was 0.2 cm thick. Finally, the steady-state rate of diffusion through the skin was obtained as the slope of the line shown in Figure 1, which gave the amount of formaldehyde resorbed per h at steady state, Q = 0.0166 mg/cm^2/h. At steady-state:

$$Q = \frac{F}{R} = \frac{C \cdot K_{s:w} \cdot D_{skin}}{d_s},$$

which was solved to obtain

$$K_{s:w} \cdot D_{skin} = \frac{Q \cdot d_s}{C} = \frac{(0.0166 \text{ mg/cm}^2/\text{hr}) \cdot (0.2 \text{ cm})}{(81.5 \text{ mg/cm}^3) \cdot (3600 \text{ s/hr})} = 1.13 \cdot 10^{-8} \text{cm}^2/\text{s}.$$

For transport across the nonmucus-coated squamous epithelium in the nose, the squamous layer was assumed to be d$_s$ = 20 μm = 0.002 cm thick. The diffusing entity was assumed to be HCH(OH)$_2$, the hydrate of formaldehyde. From Olson and Hoffmann (1989), the water:air partition coefficient (Henry's Law constant) at 25°C is

$$H^* = [HCH(OH)_2]_{aq}/[HCHO]_g = 2.97 \cdot 10^3 \text{ M/atm.}$$

After converting this number to dimensionless units using the ideal gas law, the appropriate water:air partition coefficient was found to be

$$H_w = (2.97 \cdot 10^3 \text{ M/atm}) \cdot \left(0.08206 \frac{1 \cdot \text{atm}}{\text{mole} \cdot °\text{K}} \cdot 298°\text{K}\right) = 7.26 \cdot 10^4.$$

The skin:air partition coefficient was expected to be K$_{s:a}$ = K$_{s:w}$ · H$_w$. The flux into this region is

$$Q = \frac{C_{air} \cdot K_{s:a} \cdot D_{skin}}{d_s},$$

so the mass transfer coefficient for uptake into the nonmucus-coated squamous region from the air was calculated as

$$k_{nm} = \frac{Q}{C_{air}} = \frac{K_{s:a} D_{skin}}{d_s} = \frac{H_w \cdot K_{s:w} \cdot D_{skin}}{d_s}$$

$$= \frac{(7.26 \cdot 10^4) \cdot (1.13 \cdot 10^{-8} \text{ cm}^2/\text{s})}{0.002 \text{ cm}} = 0.41 \text{ cm/sec.}$$

Mass transfer coefficient for mucus-coated epithelium. A value for the mass transfer coefficient for mucus-coated regions, k$_m$, was estimated by fitting simulated overall formaldehyde uptake by the rat nose to experimental uptake data. Patterson *et al.* (1986) exposed F344 rats to 2, 6, 15, or 50 ppm formaldehyde at a steady-state inspiratory flow rate of 135 ml/min (estimated minute volume). Overall uptake by the nasal passages was measured. The

average of the experimental uptake values (Table 1) for all exposures up to and including 15 ppm was 97%. Formaldehyde uptake was simulated using the F344 rat model at the estimated minute volume flow rate of 288 ml/min with k$_{nm}$ set to 0.41 cm/s and k$_m$ set to varying values until overall uptake by the rat nose was equal to 97%. This procedure gave a value for k$_m$ of 4.7 cm/s. The values k$_{nm}$ = 0.41 cm/s and k$_m$ = 4.7 cm/s were used for nonmucus- and mucus-coated regions, respectively, in all subsequent simulations of regional formaldehyde uptake in rat, monkey, and human noses.

Uptake and flux calculations. Overall uptake of formaldehyde was calculated as 100% × (mass entering nostril – mass exiting outlet)/(mass entering nostril). Mass balance errors for air (100% × [mass of air entering nostril − mass exiting outlet]/[mass entering nostril]) and inhaled formaldehyde (100% × [mass entering nostril − mass absorbed by airway walls − mass exiting outlet]/[mass entering nostril]) were calculated. Using the postprocessor module of FIDAP (FIPOST), flux was calculated as the rate of mass transport in the direction perpendicular to the nasal wall per mm^2 of the wall surface and thus had units of pmol/(mm^2-h-ppm). Formaldehyde flux was estimated for the rat, monkey, and human over the entire nasal surface and over the portion of the nasal surface that was lined by nonsquamous epithelium. Formaldehyde flux was also estimated for the rat and monkey over areas where cell proliferation measurements were made (Monticello *et al.,* 1989, 1991) and over the anterior portion of the human nasal passages that is lined by nonsquamous epithelium.

Mass balance errors for inhaled formaldehyde were calculated (see above) by comparing estimates for the amount of formaldehyde absorbed by airway walls in 2 ways. The amount of formaldehyde absorbed was calculated as (mass flow at the nostril – mass flow at the outlet) and separately as the mass flow in the direction perpendicular to airway walls. The mass balance error was defined as the difference between these 2 quantities. Investigations into possible causes for mass balance errors revealed that most of this error occurred as mass lost when calculating formaldehyde mass flow in the direction perpendicular to airway walls on an element-by-element basis. Estimation methods used by FIPOST for mass flow evidently contributed error to flux calculations for each element of an airway wall region. This error was largest for element-by-element calculation of flux over complex surfaces such as airway walls, and smaller for flatter surfaces such as the nostrils and outlet. The calculation of overall nasal uptake was not significantly affected by these errors since flux through airway walls was not used in this calculation. Because CFD mesh elements were roughly uniform in shape and size, mass balance errors were accounted for by evenly distributing the lost mass over the entire nasal surface and adjusting all predicted flux values accordingly.

RESULTS

Three-dimensional computer reconstructions (CFD models) of the nasal passages of rat, monkey, and human (Fig. 2) were used to simulate regional airflow and formaldehyde uptake.

TABLE 1
Uptake of Inhaled Formaldehyde Measured in the Nasal Passages of Individual F344 Rats for Various Exposure Levels

Exposure (ppm)	Animal number					Mean	SD
	1	2	3	4	5		
2	97.9	97.3	98.7	94.6	95.3	96.8	1.7
6	95.5	92.6	96.9	98.5	98.8	96.5	2.5
15	97.6	99.0	96.7	98.6	97.4	97.9	0.9
Overall						97.0	1.8

Note. Uptake of inhaled formaldehyde given as %; SD, standard deviation.
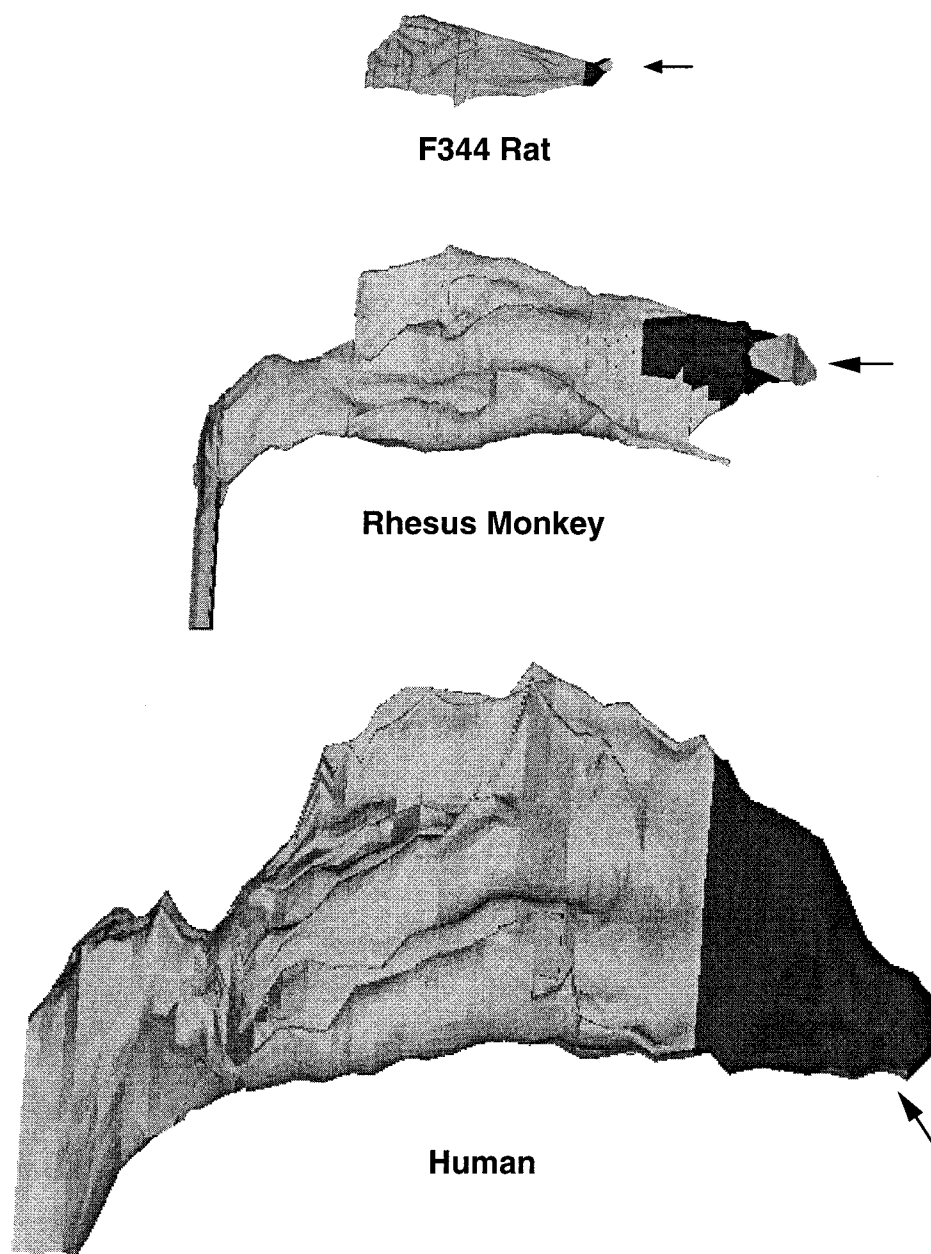
F344 Rat

Rhesus Monkey

Human
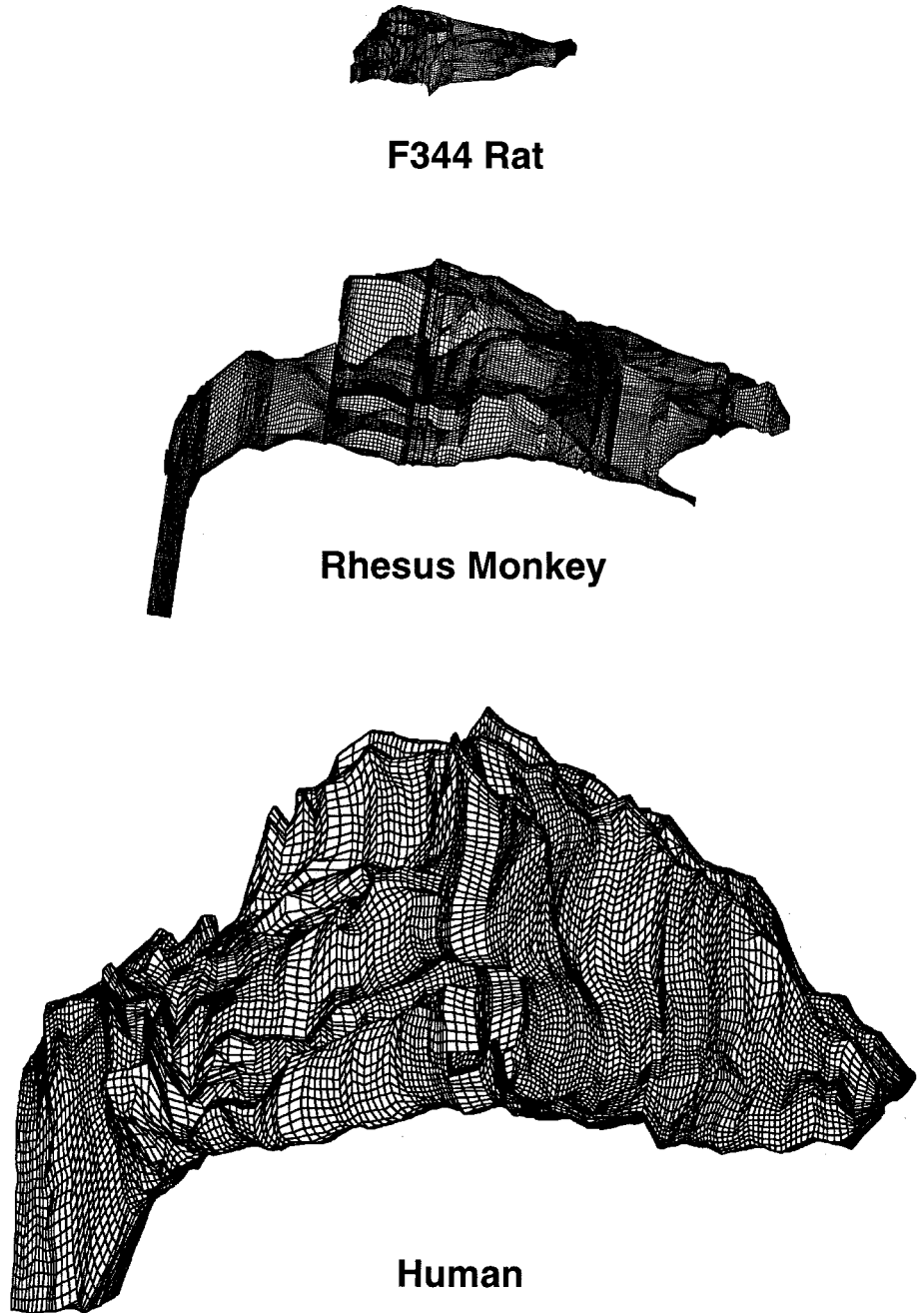
FIG. 2. Lateral views of computer reconstructions (meshes) used in computational fluid dynamics studies of nasal airflow and formaldehyde uptake. Nasal passages were reconstructed from serial step sections (rat and monkey) or magnetic resonance imaging (human). Nostrils are to the right. Plots show views at correct relative size. Modified from Kimbell *et al.* (1997a), Kepler *et al.* (1998), Subramaniam *et al.* (1998), and Kimbell *et al.* (1997c).

Each CFD model contained over 140,000 nodes or crosshairs on the nasal walls and throughout the interior air space at which simulated airflow speed and direction and formaldehyde gas concentration were obtained. The surface areas and volumes of each species' nasal passage, from nostril to outlet end, were estimated to be 1851 mm^2 and 324 mm^3 in the rat (Kimbell *et al.,* 1997a), 7170 mm^2 and 7500 mm^3 in the monkey (Kepler *et al.,* 1995), and 24,611 mm^2 and 33,100 mm^3 in the human, respectively.

Nasal surface area lined by squamous epithelium was estimated to be 187 mm^2 in the rat, 1124 mm^2 in the monkey, and 3246 mm^2 in the human. The surface area of the nonmucus-coated region as approximated from the CFD models was 72 mm^2 (4% of the total nasal surface area) in the rat, 942 mm^2 (13% of the total nasal surface area) in the monkey, and 3246 mm^2 (13% of the total nasal surface area) in the human (Fig. 3).

Simulated streamlines of steady-state inspiratory airflow agreed with experimentally observed patterns of flow in the rat and monkey and measurements of axial flow speed in the human (Fig. 4). These comparisons were described in detail previously (Kepler *et al.,* 1998; Kimbell *et al.,* 1993, 1997a;

FIG. 3. Estimated locations of non-mucus-coated squamous epithelium (dark gray) in the noses of the F344 rat, rhesus monkey, and human. Nasal passages are shown in correct relative scale; arrows indicate position of nostrils (light gray in rat and monkey, not visible due to downward orientation in human).

Subramaniam *et al.,* 1998). Errors in the mass balance of air were less than 0.4% in all simulations.

Regional uptake of inhaled formaldehyde was simulated in each species at flows equal to twice the estimated minute volume rate (Fig. 5). Overall uptake of inhaled formaldehyde by the nasal passages of each species was predicted to be 90% in the rat, 67% in the monkey, and 76% in the human. Mass balance errors for inhaled formaldehyde were 14% or less in all simulations.

Estimates of regional formaldehyde wall mass flux, averaged over a breath, are given in Table 2 for various locations in the rat, monkey, and human nasal passages. Maximum flux estimates for the entire nasal passages were located in the mucus-coated squa-

mous epithelium on the dorsal aspect of the dorsal medial meatus near the boundary between mucus- and nonmucus-coated squamous epithelium in the rat, at the anterior or rostral margin of the middle turbinate in the monkey, and in the nonsquamous epithelium on the proximal portion of the mid-septum near the boundary between squamous and nonsquamous epithelium in the human. When attention was restricted to nonsquamous-lined portions of the nose, the location of maximum flux estimates was unchanged in the monkey and human, but shifted posteriorly within the dorsal medial meatus to the nonsquamous epithelium near the boundary between squamous and nonsquamous epithelium in the rat. Flux predictions in cell proliferation sites in the rat (Monticello *et al.,* 1996) and monkey (Monticello *et al.,* 1989) were estimated to be
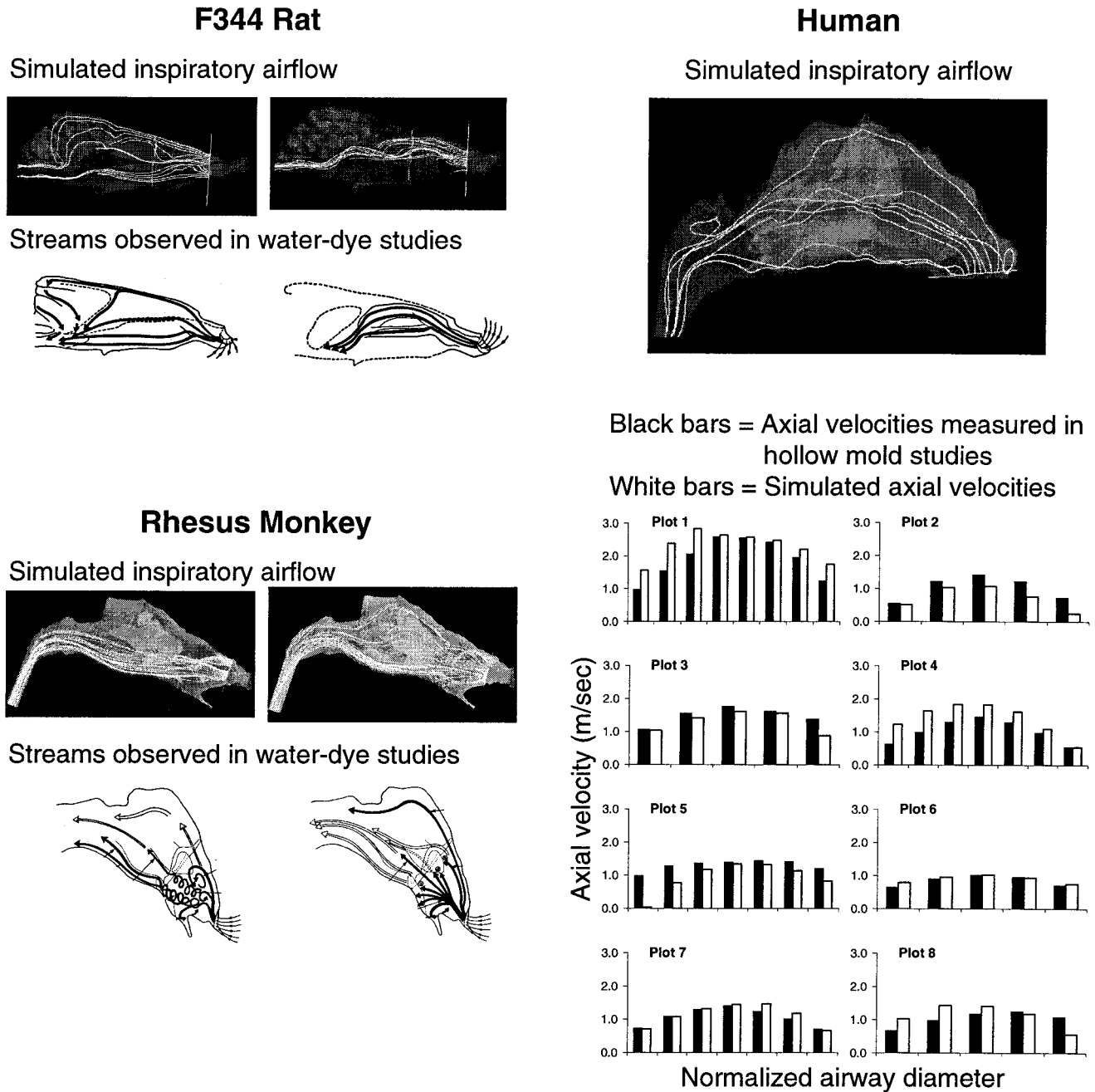
FIG. 4. Simulated inspiratory airflow patterns in the F344 rat, rhesus monkey, and human. In all cases, nostrils are to the right. Each panel shows both simulated flow patterns and experimentally observed (rat and monkey) or measured (human) airflow. Simulated streamline plots are for flows at estimated resting minute volume rates (0.288 l/min in the rat, 2.4 l/min in the monkey, 7.4 l/min in the human). Dye streakline plots were compiled for rat and monkey over the physiological range of inspiratory flow rates, and comparisons between experimental measurements and simulated results in the human were made at 15.0 l/min. Figure adapted from Kimbell *et al.* (1997a) and Morgan *et al.* (1991) for the rat, Kepler *et al.* (1998) and Morgan *et al.* (1991) for the monkey, and Subramaniam *et al.* (1998) for the human.

within 4-fold of each other, and the rat-to-monkey ratio of the highest site-specific fluxes in the 2 species was 0.98.

In the rat, the incidence of formaldehyde-induced squamous cell carcinoma in chronically exposed animals was high in the anterior lateral meatus (Monticello *et al.,* 1996). Flux predicted per ppm in this site and flux predicted near the anterior or proximal aspect of the inferior turbinate and adjacent lateral walls and septum in the human were similar, with a rat-value-to-human-value ratio of 0.84.

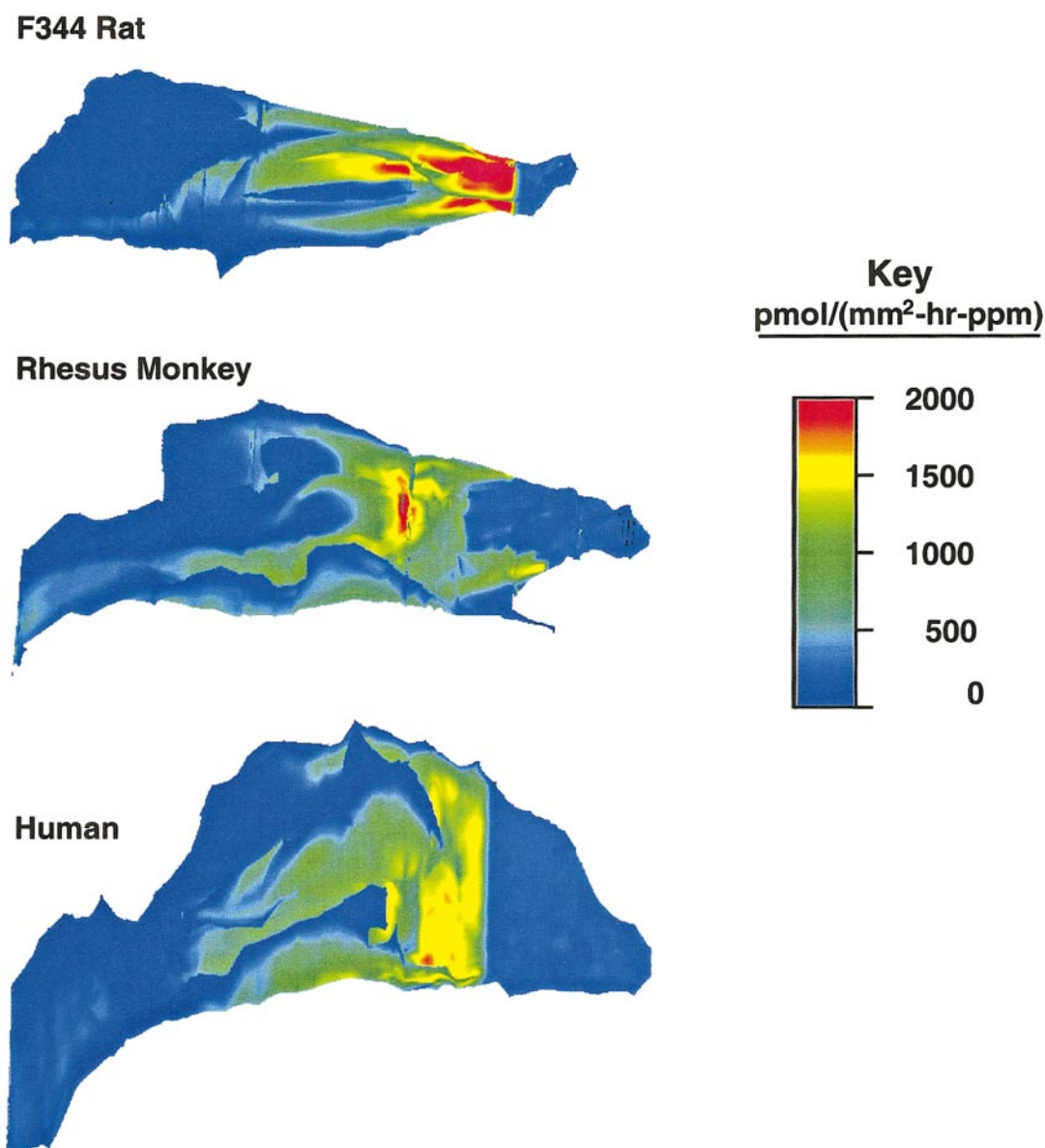The maximum estimated wall mass flux of formaldehyde

F344 Rat

Rhesus Monkey

Key
pmol/(mm²-hr-ppm)

2000

1500

1000

500

0

Human

FIG. 5. Lateral view of nasal wall mass flux of inhaled formaldehyde simulated in each species at steady-state inspiratory flow rates of 0.576 l/min in the rat, 4.8 l/min in the monkey, and 15 l/min in the human. In each case, flux has been contoured over the range from 0 to 2000 pmol/(mm²-h-ppm). Nostrils are to the right.

averaged over the breathing cycle, for nonsquamous epithelium of each species was 2620 pmol/(mm²-h-ppm) in the rat, 4492 pmol/(mm²-h-ppm) in the monkey, and 2082 pmol/(mm²-h-ppm) in the human.

DISCUSSION

Experimental determination of local formaldehyde uptake patterns is severely limited in the nasal passages. Low resolution of dissection techniques and the rapidity of formaldehyde metabolism and reactivity make direct assessment of formaldehyde uptake patterns very difficult, especially for comparison among different species. The CFD models described here allow researchers to predict local formaldehyde concentrations and fluxes throughout the nasal passages. These simulations can be used to test hypotheses about mechanisms of formaldehyde toxicity as well as to make comparisons of formaldehyde uptake patterns that capture species-specific differences among rats, monkeys, and humans for risk assessment purposes.

The development and use of CFD models for nasal formaldehyde uptake required a number of assumptions regarding anatomical, parameter estimation, and simulation issues. Fac-

TABLE 2
Estimates of Formaldehyde Flux at Nasal Passage Walls

Nasal region	Formaldehyde flux estimate (pmol/[mm²-h-ppm])		
	Rat	Monkey	Human
Whole nose: average	336	508	568
Whole nose: maximum	3210	4492	2082
Nonsquamous: average	284	535	611
Nonsquamous: maximum	2620	4492	2082
Cell proliferation sites	ALM: 825	Level B: 845	NA
	PLM: 551	Level C: 544	
	ADS: 503	Level D: 197	
	MMT: 584	Level E: 249	
	AMS: 730		
	PMS: 548		
AIT & ALWS	NA	NA	988

Note. Rat: ALM, anterior lateral meatus; PLM, posterior lateral meatus; ADS, anterior dorsal septum; MMT, medial maxilloturbinate; AMS, anterior mid-septum; PMS, posterior mid-septum (Monticello *et al.,* 1996). Monkey: as described by Monticello and colleagues (1989). NA, not applicable. AIT & ALWS, anterior aspect of the inferior turbinate and adjacent lateral walls and septum.

tors that were not included in these models such as the presence of other inhaled species, the presence of water vapor, the nasal cycle, and the relative lengths of inspiration and expiration times may affect formaldehyde uptake. However, there is insufficient information on the degree to which most of these factors affect uptake to include them in the CFD models at this time. In addition, DPX predictions based on formaldehyde flux that did not account for these factors agreed with experimental data, suggesting that error introduced by the exclusion of these factors was insignificant at the current level of experimental measurements. The assumptions and parameters to which simulation results are expected to be most sensitive are (1) the use of individual monkey and human nasal anatomies as representatives of the general population, (2) the location and extent of squamous epithelium and of mucus- and nonmucus-coated nasal regions in the human, and (3) the values of the mass transfer coefficients.

Quantification of anatomical sources of uncertainty involves determining the extent to which normal variations in these model inputs affect regional flux predictions. To determine variation in respiratory anatomy, new models based on a variety of monkey and human individuals need to be developed. In addition, potential effects on formaldehyde flux predictions from the use of fixed tissue specimens to represent in-life nasal passages need to be assessed. Detailed mapping using light microscopy on step-sectioned human specimens could be conducted to determine the location, surface area, and thickness of human nasal epithelial types.

The calculation of the mass transfer coefficient for nonmucus-coated epithelium, k_{nm}, was based on an estimation of 20

μm for the thickness of squamous epithelium in the nasal vestibule. This value of k_{nm} was used in all CFD simulations. Squamous thickness in the monkey nasal vestibule is probably larger than 20 μm, based on examination of histological slides of control rhesus monkey nasal tissue. A squamous thickness greater than 20 μm leads to a lower value for k_{nm} that would account for less formaldehyde uptake in the nasal vestibule and lead to more formaldehyde uptake in posterior, mucus-coated regions. Thus monkey and human nasal fluxes in mucus-coated regions may be underestimated in the simulations presented here. Simulations using the monkey CFD model with k_{nm} adjusted 3-fold lower than the value used in the predictions reported here indicated that regional fluxes in mucus-coated regions changed by less than 5%.

Qualitatively, the formaldehyde flux patterns reported here for the rat and monkey agreed with patterns previously described by Kimbell *et al.* (1993) for the anterior rat nose and the monkey nose (Kepler *et al.,* 1998), except in the dorsal medial meatus of the rat. In this region, fluxes predicted by the simulation described here were higher than those estimated by simulations described by Kimbell *et al.* (1993). This discrepancy persisted after reducing the faster airflow rate of current uptake calculations to match earlier estimates and is most likely due to the use of a mesh in which the nasal vestibule has a different shape from that of earlier simulations (Kimbell *et al.,* 1997b).

Monticello and colleagues measured formaldehyde-induced cell proliferation rates in several locations in the noses of rats (Monticello *et al.,* 1991) and monkeys (Monticello *et al.,* 1989) exposed to 6 ppm formaldehyde for 6 weeks. They reported similar increases in cell proliferation rates over control values for the 2 species, with rats showing 2- to 16-fold increases and monkeys showing 9- to 20-fold increases. Formaldehyde flux predicted in these sites using rat and monkey CFD models indicated that flux values in rat and monkey sites were also similar, with a rat-to-monkey ratio of 0.98 for highest site-specific flux values and other site-specific values predicted to be within 4-fold of each other. These results show that predicted formaldehyde flux in cell proliferation measurement sites is consistent with formaldehyde-induced cell proliferative responses in both the rat and monkey, and further support the hypothesis that formaldehyde flux is a key player in determining toxic response.

Formaldehyde uptake simulations using the human CFD model predicted that flux values in a region containing the anterior aspect of the inferior turbinate and adjacent lateral walls and septum were similar to fluxes predicted in rat and monkey cell proliferation measurement sites. This result suggests that similar cell proliferative and carcinogenic responses could be expected to occur in humans exposed to formaldehyde under conditions similar to those inducing these responses in rats and monkeys.

Clonal growth models for carcinogenesis require information on cell birth, death, and mutation rates (Cohen and Ell-

wein, 1990; Moolgavkar and Venzon, 1979). Measurements or estimates of these rates can be made from cell proliferation and DPX data gathered from specific sites in the nasal passages. Variations in these data by site indicate that no single site-specific value can represent the entire tissue (Casanova *et al.,* 1991, 1994; Monticello *et al.,* 1989, 1996). If cell proliferation or DPX formation rates are linked to predictions of regional formaldehyde flux, however, flux predicted throughout the nasal passages via CFD modeling can be used to extrapolate data estimating cell birth, death, and mutation rates from measurement sites to the rest of the nasal passages. In addition, the use of CFD modeling based on anatomically realistic nasal geometry allows this extrapolation to incorporate species-specific variations in formaldehyde uptake patterns and hence local cell proliferation and DPX formation rates within the nasal passages. Species-specific patterns of nasal cell proliferation and DPX formation rates can be incorporated into clonal growth modeling by partitioning each species' nasal passage into zones where cell proliferation and DPX formation rates are based on an average flux for that zone. A clonal growth model can then be run separately for each zone and predicted zonal cancer risks aggregated to provide an estimate of overall nasal cancer risk.

In summary, 3-dimensional, anatomically accurate, CFD models of airflow and inhaled formaldehyde gas uptake in the nasal passages of a rat, monkey, and human provide valuable insight into mechanisms of local nasal dosimetry for inhaled water-soluble gases. Estimates of regional nasal formaldehyde flux, including maximum flux, average flux, and flux in specific nasal regions, were compared among the 3 species. These results serve as input for risk modeling of formaldehyde carcinogenesis to help reduce uncertainty in human cancer risk estimates from formaldehyde exposure.

ACKNOWLEDGMENTS

REFERENCES

Andersen, M. E., Sarangapani, R., Frederick, C. B., and Kimbell, J. S. (1999). Dosimetric adjustment factors for methyl methacrylate derived from a steady-state analysis of a physiologically based clearance-extraction model. *Inhal. Toxicol.* **11,** 899–926.

Batchelor, G. K. (1967). *An Introduction to Fluid Dynamics.* Cambridge University Press, Cambridge, UK.

Bogdanffy, M. S., Sarangapani, R., Kimbell, J. S., Frame, S. R., and Plowchalk, D. R. (1998). Analysis of vinyl acetate metabolism in rat and human nasal tissues by an *in vitro* gas uptake technique. *Toxicol. Sci.* **46,** 235–246.

Bush, M. L., Frederick, C. B., Kimbell, J. S., and Ultman, J. S. (1998). A CFD-PBPK hybrid model for simulating gas and vapor uptake in the rat nose. *Toxicol. Appl. Pharmacol.* **150,** 133–145.

Casanova, M., Deyo, D. F., and Heck, H. d'A. (1989). Covalent binding of inhaled formaldehyde to DNA in the nasal mucosa of Fischer 344 rats: Analysis of formaldehyde and DNA by high-performance liquid chromatography and provisional pharmacokinetic interpretation. *Fundam. Appl. Toxicol.* **12,** 397–417.

Casanova, M., Morgan, K. T., Gross, E. A., Moss, O. R., and Heck, H. d'A. (1994). DNA-protein cross-links and cell replication at specific sites in the nose of F344 rats exposed subchronically to formaldehyde. *Fundam. Appl. Toxicol.* **23,** 525–536.

Casanova, M., Morgan, K. T., Steinhagen, W. H., Everitt, J. I., Popp, J. A., and Heck, H. d'A. (1991). Covalent binding of inhaled formaldehyde to DNA in the respiratory tract of rhesus monkeys: Pharmacokinetics, rat-to-monkey interspecies scaling, and extrapolation to man. *Fundam. Appl. Toxicol.* **17,** 409–428.

Cohen, S. M., and Ellwein, L. B. (1990). Cell proliferation in carcinogenesis. *Science* **249,** 1007–1011.

Cohen Hubal, E. A., Kimbell, J. S., and Fedkiw, P. S. (1996). Incorporation of nasal-lining mass-transfer resistance into a CFD model for prediction of ozone dosimetry in the upper respiratory tract. *Inhal. Toxicol.* **8,** 831–857.

Cohen Hubal, E. A., Schlosser, P. M., Conolly, R. B., and Kimbell, J. S. (1997). Comparison of inhaled formaldehyde dosimetry predictions with DNA-protein cross-link measurements in the rat nasal passages. *Toxicol. Appl. Pharmacol.* **143,** 47–55.

Conolly, R. B., Lilly, P. D., and Kimbell, J. S. (2000). Simulation modeling of the tissue disposition of formaldehyde to predict nasal DNA-protein cross-links in Fischer 344 rats, rhesus monkeys, and humans. *Environ. Health Perspect.* **108**(Suppl.), 919–924.

Frederick, C. B., Bush, M. L., Lomax, L. G., Black, K. A., Finch, L., Kimbell, J. S., Morgan, K. T., Subramaniam, R. P., Morris, J. B., and Ultman, J. S. (1998). Application of a hybrid computational fluid dynamics and physiologically based inhalation model for interspecies dosimetry extrapolation of acidic vapors in the upper airways. *Toxicol. Appl. Pharmacol.* **152,** 211–231.

Godo, M. N., Morgan, K. T., Richardson, R. B., and Kimbell, J. S. (1995). Reconstruction of complex passageways for simulations of transport phenomena: Development of a graphical user interface for biological applications. *Comp. Meth. Prog. Biomed.* **47,** 97–112.

Guyton, A. C. (1947) Measurement of the respiratory volumes of laboratory animals. *Am. J. Physiol.* **150,** 70–77.

Harkema, J. R. (1992). Epithelial cells of the nasal passages. In *Comparative Biology of the Normal Lung.* (R. A. Parent, Ed.), pp. 27–36. CRC Press, Boca Raton, FL.

Harkema, J. R., Plopper, C. G., Hyde, D. M., St. George, J. A., Wilson, D. W., and Dungworth, D. L. (1987). Response of the macaque nasal epithelium to ambient levels of ozone: A morphologic and morphometric study of the transitional and respiratory epithelium. *Am. J. Pathol.* **128,** 29–44.

Heck, H. d'A., Casanova, M., and Starr, T. B. (1990). Formaldehyde toxicity—new understanding. *Crit. Rev. Toxicol.* **20**(6), 397–426.

Hobler, T. (1966). *Mass Transfer and Absorbers.* Pergamon Press, New York.

ICRP66 (1994). Human Respiratory Tract Model for Radiological Protection. In *Annals of the ICRP*, Vol. 24, (1–3). Publication 66. International Commission on Radiological Protection. Elsevier Science, Tarrytown, NY.

Kepler, G. M., Joyner, D. R., Fleishman, A., Godo, M. N., Richardson, R. B., Gross, E. A., Morgan, K. T., and Kimbell, J. S. (1995). Method for obtaining accurate geometrical coordinates of nasal airways for computer dosimetry modeling and lesion mapping. *Inhal. Toxicol.* **7,** 1207–1224.

Kepler, G. M., Richardson, R. B., Morgan, K. T., and Kimbell, J. S. (1998). Computer simulation of inspiratory nasal airflow and inhaled gas uptake in a rhesus monkey. *Toxicol. Appl. Pharmacol.* **150,** 1–11.

Kerns, W. D., Pavkov, K. L., Donofrio, D. J., Gralla, E. J., and Swenberg, J. A. (1983). Carcinogenicity of formaldehyde in rats and mice after long-term inhalation exposure. *Cancer Res.* **43,** 4382–4392.

Kimbell, J. S., Godo, M. N., Gross, E. A., Joyner, D. R., Richardson, R. B., and Morgan, K. T. (1997a). Computer simulation of inspiratory airflow in all regions of the F344 rat nasal passages. *Toxicol. Appl. Pharmacol.* **145,** 388–398.

Kimbell, J. S., Gross, E. A., Joyner, D. R., Godo, M. N., and Morgan, K. T. (1993). Application of computational fluid dynamics to regional dosimetry of inhaled chemicals in the upper respiratory tract of the rat. *Toxicol. Appl. Pharmacol.* **121,** 253–263.

Kimbell, J. S., Gross, E. A., Richardson, R. B., Conolly, R. B., and Morgan. K. T. (1997b). Correlation of regional formaldehyde flux predictions with the distribution of formaldehyde-induced squamous metaplasia in F344 rat nasal passages. *Mutat. Res.* **380,** 143–154.

Kimbell, J. S., Subramaniam, R. P., and Miller, F. J. (1997c). Computer models of nasal airflow and inhaled gas uptake in the rat, monkey, and human: Implications for interspecies dosimetry. *CIIT Activities* **17**(11), 1–7.

Lodén, M. (1986). The *in vitro* permeability of human skin to benzene, ethylene glycol, formaldehyde, and n-hexane. *Acta Pharmacol. Toxicol.* **58,** 382–389.

Mauderly, J. L. (1986). Respiration of F344 rats in nose-only inhalation exposure tubes. *J. Appl. Toxicol.* **6,** 25–30.

Monticello, T. M., Miller, F. J., and Morgan, K. T. (1991). Regional increases in rat nasal epithelial cell proliferation following acute and subchronic inhalation of formaldehyde. *Toxicol. Appl. Pharmacol.* **111,** 409–421.

Monticello, T. M., Morgan, K. T., Everitt, J. I., and Popp, J. A. (1989). Effects of formaldehyde gas on the respiratory tract of rhesus monkeys: Pathology and cell proliferation. *Am. J. Pathol.* **134,** 515–527.

Monticello, T. M., Swenberg, J. A., Gross, E. A., Leininger, J. R., Kimbell, J. S., Seilkop, S., Starr, T. B., Gibson, J. E., and Morgan, K. T. (1996).

Correlation of regional and nonlinear formaldehyde-induced nasal cancer with proliferating populations of cells. *Cancer Res.* **56,** 1012–1022.

Moolgavkar, S. H. and Venzon, D. J. (1979). Two-event models for carcinogenesis: Incidence curves for childhood and adult tumors. *Math. Biosci.* **47,** 55–77.

Morgan, K. T., Gross, E. A., and Patterson, D. L. (1986a). Distribution, progression, and recovery of acute formaldehyde-induced inhibition of nasal mucociliary function in F-344 rats. *Toxicol. Appl. Pharmacol.* **86,** 448–456.

Morgan, K. T., Jiang, X. Z., Patterson, D. L., and Gross, E. A. (1984). The nasal mucociliary apparatus. Correlation of structure and function in the rat. *Am. Rev. Resp. Dis.* **130,** 275–281.

Morgan, K. T., Jiang, X. Z., Starr, T. B., and Kerns, W. D. (1986b). More precise localization of nasal tumors associated with chronic exposure of F-344 rats to formaldehyde gas. *Toxicol. Appl. Pharmacol.* **82,** 264–271.

Morgan, K. T., Kimbell, J. S., Monticello, T. M., Patra, A. L., and Fleishman, A. (1991). Studies of inspiratory airflow patterns in the nasal passages of the F-344 rat and rhesus monkey using nasal molds: Relevance to formaldehyde toxicity. *Toxicol. Appl. Pharmacol.* **110,** 223–240.

Mygind, N., Pedersen, M., and Nielsen, M. H. (1982). Morphology of the upper airway epithelium. In *The Nose, Upper Airway Physiology and the Atmospheric Environment.* (D. F. Proctor and I. Andersen, Eds.), pp. 71–97. Elsevier Biomedical Press, New York.

Olson, T. R. and Hoffmann, M. R. (1989). Hydroxyalkylsulfonate formation: Its role as an S(IV) reservoir in atmospheric water droplets. *Atmos. Environ.* **23,** 985–997.

Patterson, D. L., Gross, E. A., Bogdanffy, M. S., and Morgan, K. T. (1986). Retention of formaldehyde gas by the nasal passages of F-344 rats. *Toxicologist* **6,** 55.

Subramaniam, R. P., Richardson, R. B., Morgan, K. T., Guilmette, R. A., and Kimbell, J. S. (1998). Computational fluid dynamics simulations of inspiratory airflow in the human nose and nasopharynx. *Inhal. Toxicol.* **10,** 91–120.